SANDIA REPORT
SAND2023-10667R
Printed September 2023

Sandia National Laboratories

Photon Doppler Velocimetry to Spatially Resolve Plasma Density in a Power Flow Gap

Jacob T. Banasek, Pablo A. Reyes, Daniel H Dolan
Sandia National Laboratories
P.O. Box 5800, MS-1195
Albuquerque, NM 87185
jtbanas@sandia.gov

Prepared by
Sandia National Laboratories
Albuquerque, New Mexico 87185
Livermore, California 94550

Issued by Sandia National Laboratories, operated for the United States Department of Energy by National Technology & Engineering Solutions of Sandia, LLC.

Available to DOE and DOE contractors from

U.S. Department of Energy
Office of Scientific and Technical Information
P.O. Box 62
Oak Ridge, TN 37831

Telephone: (865) 576-8401
Facsimile: (865) 576-5728
E-Mail: reports@osti.gov
Online ordering: http://www.osti.gov/scitech

Available to the public from

U.S. Department of Commerce
National Technical Information Service
5301 Shawnee Road
Alexandria, VA 22312

Telephone: (800) 553-6847
Facsimile: (703) 605-6900
E-Mail: orders@ntis.gov
Online order: https://classic.ntis.gov/help/order-methods

ABSTRACT

The understanding of power flow plasmas is important as we look towards next generation pulsed power (NGPP) as current losses could prohibit the goals of that facility. Therefore, it is important to have accurate diagnostics of the plasma parameters on the current machines, which can be used to help inform and improve simulations. Having these plasma parameters will help validate models and simulations to provide confidence when they are expanded to conditions relevant to NGPP. One important plasma parameter that can be measured is the electron density, which can be measured by photonic Doppler velocimetry (PDV). A PDV system has several key advantages over other interferometers by measuring relatively low densities ($> 1 \times 10^{15}$ cm^{-2}) with both spatial and temporal resolution. Experiments were performed on the Mykonos pulsed power machine, which is a 1 MA sub scale machine in which recent platforms have been developed to explore current densities relevant to the inner magnetically insulated transmission line (MITL) on the Z machine. Experiments were performed on two different platforms, the thin foil platform and the Mykonos parallel plate platform (MP3). In addition, a combination of both single-point and multi-point measurements were used. The single-point measurements proved to be very promising, providing a clear increase in density at about 70 ns into the current rise on thin foil experiments up to about 5×10^{17} cm^{-3} before the probe stopped providing signal. While we did also see returns from multi-point measurements on both platforms, the signals were not as easy to interpret due to strong background effects. However, they do show initial promise for this diagnostic to measure density at several points across a 1 mm gap. These measurements provide insights in how to improve the diagnostic so that it can provide useful information on power flow relevant experiments.

ACKNOWLEDGMENT

First we could not have tested this diagnostic with out being able to field it as a ride along on both Trevor Smith and Derek Lamppa experiments. We appreciate both of them giving use some of the valuable lines of sight on their platform, as well es experimental time so that we could setup and test this diagnostic.

We also greatly appreciate all the help from Sheri Payne, for help in learning how to run and use the PDV system. As well as providing the PDV system for us to use.

Thanks to Mike Cuneo for help in developing the initial idea, and for Keith Matzen for funding the project and many useful discussions.

CONTENTS

LIST OF FIGURES

This page left blank

1. INTRODUCTION

One important question as Sandia looks towards a next generation pulsed power (NGPP) facility is the importance of current losses on a larger scale machine then Z. While current loss is relevant to Z, we are still able to deliver a decent fraction of the current to the load. The question though is when the machine is scaled up to around 60 MA pulse, as is the goal for NGPP, do these losses become more important and potentially cause NGPP to be prohibitive. Since we cannot reach exact NGPP conditions on the machines currently available to use, it is important to have accurate models to predict what will happen on a larger scale machine. To ensure our models are accurate they need to be compared to experiments performed on either Z or smaller sub scale facilities. To compare experimental plasmas to the models it is important to have accurate diagnostics of various plasma parameters.

One plasma parameter that is of keen interest is the electron density, which tells us the location and amount of plasma. For power flow it is important to know where and when the plasma forms across the anode cathode (AK) gap, as that plasma can lead to current loss. To achieve this, it is desirable to have both a temporally and spatially resolved interferometer system to measure the changing density of the plasma.

A common interferometer technique on pulsed power plasmas is using green laser light to form an imaging interferometer, such as in a Mach-Zehnder arrangement. While this creates very good spatial information of the plasma density, it has limited temporal information, as it can only perform measurements at the time of the laser pulse. Another challenge of this green interferometry is that for 532 nm wavelength a single fringe shift corresponds to a density of 4×10^{17} cm^{-2}, limiting the capability to measure low electron densities.

There has also been recent development of a dispersion interferometer [5]. This has the advantages of both relatively low density measurements, down to 1×10^{14} cm^{-2} and temporal resolution of the plasma density. However, at least as currently arranged, it does not have an easy path to spatial resolution of the electron density in a signal experiment.

Therefore, we have decided to look to photonic Doppler velocimetry (PDV) as a possibility to study the plasma in the AK gap. PDV is typically used to measure the velocity of various targets[2]. PDV has a key advantage over other interferometer techniques as it can be completely contained within fibers, other than right near the load, making it relatively easy to set up as it is self-contained. Recent research has shown that it is capable of measuring the electron density instead of velocity [3, 10]. Since the entire delivery is contained within fibers, the limitation on the spatial resolution is driven by the focusing of the fibers. In addition, this diagnostic provides temporal resolution of the density. Finally, as is detailed in this report, it is capable of measuring densities down to $\sim 7 \times 10^{14}$ cm^{-2} which is lower than the capabilities of interferometry at 532 nm. Therefore, this diagnostic can provide density information needed to compare power flow plasmas to simulations. The main focus of this work was to expand on previous work done to measure the electron density using PDV, but now applying those principles to a higher spatially resolved scale as well as applying the diagnostic to power flow plasmas [3, 10].

This diagnostic was developed on the Mykonos pulsed power accelerator, which is a 1 MA pulsed power machine. This machine was chosen to develop the diagnostic on as being a sub scale

machine it is easier for development as experimental time is more available then on Z. In addition, there has been recent developments of a platform that both enables easy diagnostic access as well as reaching current densities equivalent to inside the inner magnetically insulated transmission lines (MITLs). The inner MITLs are a prime location for current loss on Z, and therefore being able to study a similar current density on a subscale facility is a great opportunity to develop this diagnostic.

2. PDV DIAGNOSTIC

Photonic Doppler Velocimetry (PDV) is a heterodyne interferometry technique used primarily to measure the velocity of various surfaces [9]. This diagnostic is often used in similar situations as VISAR (Velocity interferometer system for any reflector). A full review of the various methods and techniques to perform PDV measurements was recently published by Dolan [2]. Here we will provide an overview of the PDV techniques relevant to this work, and how PDV can be used for density measurements.

2.1. How PDV works

PDV works as an interferometer by measuring the difference in frequency between the probing laser and a reference laser. This reference laser can either be some fraction of the probe laser, or as is the case in these experiments, be a separate laser that is slightly detuned from the probe laser. Using two different lasers as well as using them at different frequencies has several key advantages. The first being the adjustment of the relative power between the probe and the reference laser. Often one wants the reference laser to have significantly more power than the probe laser to reduce the influence of changes in reflectance of the probe beam on the result. In addition, having them slightly detuned enables there to be a beat frequency even when no signal is present. This is important as it makes it easy to set the intensity of the digitizer. Starting from a non-zero frequency also enables the detection of the direction of motion, as the frequency can either be up or down shifted during the experiment.

In traditional PDV changes in the beat frequency between the probe beam and the reference beam gives a measure of the velocity of the reflecting surface, v, by,

$$f_b = \left| f_0 + 2\frac{v(t)}{\lambda} \right|. \tag{1}$$

Where f_0 is the frequency difference between the probe and the reference and λ is the wavelength of the probe beam. For these experiments f_0 was about 2 GHz and a frequency change of 100 MHZ corresponds to a speed of 77.5 m/s.

To find the beat frequency of the signal the data was processed using short-time Fourier-transforms (STFT). The methods to analyze this data were a part of the Sandia Matlab AnalysiS Hierarchy Toolbox called SMASH. The STFT was centered about a point in the PDV single with a width of τ, and some windowing function. We used the "Hann" window here as it performs best for high frequency signals. Data here was analyzed with a width of 10 ns, and a time step of 1 ns. This oversampling helps to smooth the analyzed signal.

The minimum error in the velocity measurements of PDV has been found to be a function of 3 factors, the signal to noise ratio (σ_s/A), the collection rate of the scope (f_s), and the length of time of the STFT, (τ) with a minimum error of [1]

$$\sigma_f \geq \sqrt{\frac{6}{f_s \tau^3}} \frac{\sigma_s}{A} \frac{1}{\pi}. \tag{2}$$

We see from this that increasing the time window of the STFT can significantly increase the accuracy of the velocity measurement, however this sacrifices the temporal resolution of the measurement. This error can then be related to velocity from (1) and for τ=10 ns, f_s = 10 GhZ, and σ_s/A = 20 % the minimum error for velocity is 1.2 m/s. We see therefore that PDV can make highly accurate measurements of the velocity of a surface.

2.2. PDV as a density measurement

In addition to using PDV to measure the velocity, it can also measure the electron density. This is because the rate of change of the index of refraction can be treated as an apparent velocity (v^*),

$$v^*(t) \approx -L\frac{d\hat{n}}{dt}. \tag{3}$$

With L being the length scale of the plasma and $\hat{n}$ is the averaged refractive index over that length scale. By integrating this we can find the refractive index at a moment in time

$$\hat{n}(t) \approx 1 - \frac{1}{L}\int_0^t v^*(t)dt. \tag{4}$$

Since the refractive index is define as ck/ω, with k as the wavevector of the laser, and ω is the frequency of the laser, and assuming that the magnetic field is small enough to not significantly affect the radiation (discussed more later), using the dispersion relation for a light wave results in

$$\hat{n} = \sqrt{1 - \frac{\omega_{pe}^2}{\omega^2}} = \sqrt{1 - n_e/n_c}. \tag{5}$$

Where $\omega_{pe} = \sqrt{4\pi n_e e^2/m_e}$ is the plasma frequency and n_c is the critical density, which is 4.6×10^{20} cm^{-3} for λ = 1550 nm. Rearranging this therefor gives the electron density in terms of the refractive index

$$n_e(t) = n_c(1 - \hat{n}(t)^2). \tag{6}$$

And therefore, from the integration of the velocity we can use the beat frequency from the laser as a measure of the electron density of the plasma.

One key assumption in this derivation was the fact that the magnetic fields were small, and therefore we could use a dispersion model assuming no magnetic field instead of a more complicated dispersion model. To show that this is a valid assumption for these plasmas we look at changes in index of refraction between the nonmagnetic field wave and the X mode wave. Using a magnetic field of 200 T, a density of 1×10^{18} cm^{-3} and an ionization state of 3 for Aluminum results in less than 0.0001 % error between the index of refraction for the two modes for 1550 nm light. Therefore, we can be safe in ignoring the magnetic field.

There are two major sources of error in these experiments, the velocity measurements from fitting the frequency from the PDV and the errors from the measurement of the length of the plasma volume. As already discussed, the minimum error in velocity for this system is 1.2 m/s. Through

integration this can be related to an error in the density, which gives an error of 4×10^{15} cm^{-3} after integrating over 50 ns assuming a 2 mm path length.

The other major source of error is that of the integration path length. This is likely the primary source of error in the experiment, as changes in the path length of the integration directly effects the scale factor L. If this is the dominant source of error, it will propagate almost directly to the final result.

This page left blank

3. EXPERIMENTAL SET UP

3.1. Mykonos

These experiments were performed on the Mykonos pulsed power machine. Mykonos is a linear transformer driver (LTD) that can reach peak currents up to about 1 MA with a rise time of 100 ns. This machine was chosen to develop and test this diagnostic as there are several key advantages of developing this diagnostic on a subscale machine. First, the demand on shot time is much lower on Mykonos compared to Z, meaning that users can request several week campaigns instead of one or two shots, enabling testing and improving the diagnostic between shots. In addition, Mykonos is a much smaller facility making it easier to bring up and test a new diagnostic. In addition, there has been recent development of platforms on Mykonos that can reach current densities relevant to the inner MITLs on Z, meaning that it can still perform experiments on power flow physics relevant to Z. These platforms also have very good diagnostic axis, which is needed for a line-of-sight diagnostic like PDV.

The first platform was for thin foil experiments and was developed to help study power flow relevant physics on smaller scale machines. This platform was first used on the MAIZE facility and has recently been expanded to the Mykonos machine [8]. A sample of this hardware for Mykonos is shown in Fig. 3-1. It is primarily made up of dielectric, while the inner power flow surface is covered in a thin foil. The PDV diagnostic was fielded with the foil being either stainless steel or aluminum and the thicknesses were between 100 and 300 μm. Also, the AK gap is relatively large, 5 mm, making it easy to align the probe into the gap. The width of the AK gap is 5 mm, resulting in a 1 cm integration length for the interferometer, which enables measuring lower density plasma then the next platform discussed. Therefore, this is a great platform for initial testing and developing of the diagnostic.

While the thin foil platform was great for initial testing of the diagnostic the primary goal was to field this on the Mykonos Parallel Plate Platform (MP3)[6]. Fielding a multi-point measurement on this platform was the primary goal of this experiment as this platform enables the current density to reach values comparable to the inner MITL on Z, the platform was designed to provide very good diagnostic access and is a platform that various surface treatment techniques are being used to see the effect on the formation of power flow plasmas. This platform is shown in Fig. 3-2. To reach the current densities relevant to the inner MITL of Z an AK gap of 1 mm or smaller is normally used. This set a limit on how far apart our probes could be. Since we had a digitizer with 4 channels (discussed later in this section) this set the goal for our diagnostic, of fitting 4 probes within a 1 mm AK gap. This platform also has a smaller integration length then the thin foil platform of only 2 mm, limiting the density that can be measured. This integration length along the diagnostic line of sight drove the error bars that were discussed earlier. And while this small integration length limits the minimum density that can be measured, it is needed to drive the current densities up to conditions relevant to the Z inner MITL.

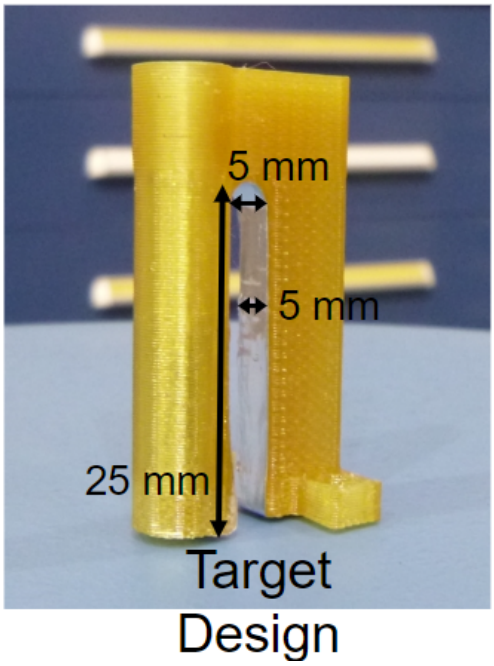

Figure 3-1 Picture of the thin foil load hardware for Mykonos.

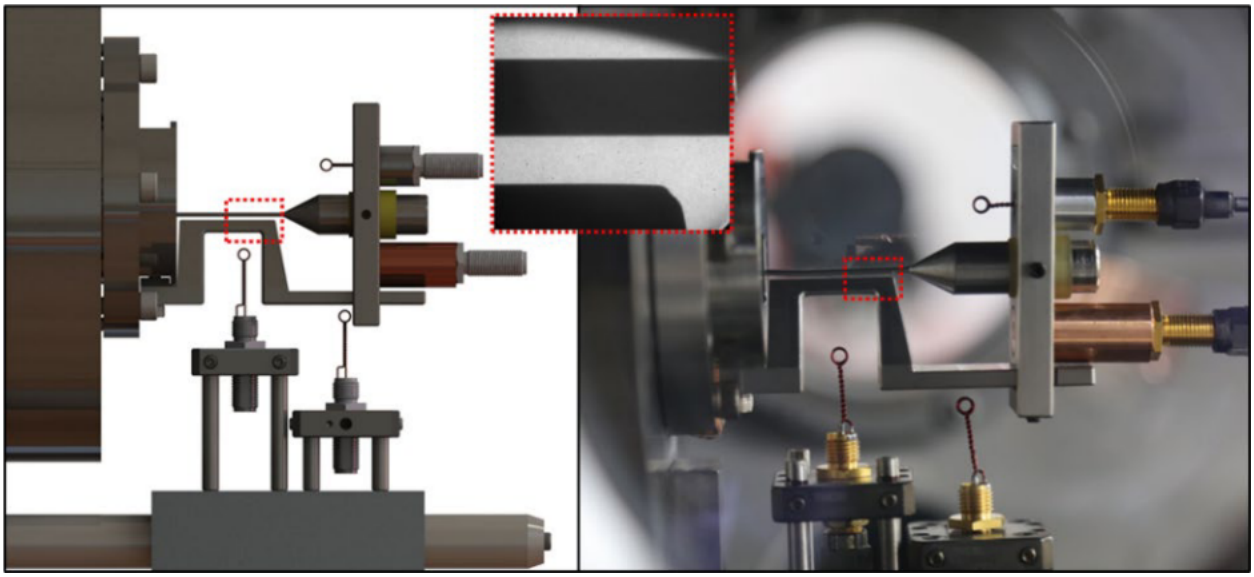

Figure 3-2 Model (left) and as-built (right) of the side-view of 0.5 mm AK gap. The cathode is on the top and the anode is the bottom. Power flow goes left to right though the cathode. This is figure 11 from [6].

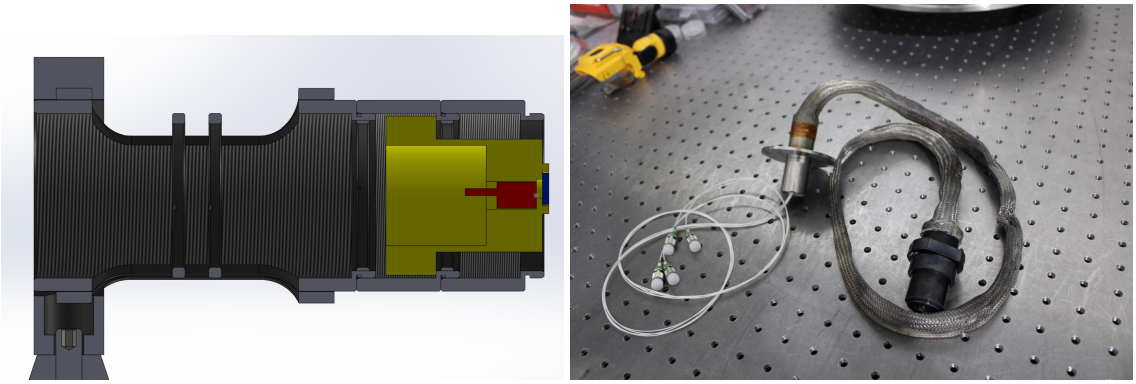

Figure 3-3 left) diagram of the mount for the PDV fiber. To hold the fiber array (red) we built a 3D printed holder (yellow), with 1550 nm coated glass window in the front (blue). The parts were held together using off the shelf 1" Thorlabs lens tube hardware. right) image of the PDV holder with the fibers mounted in it.

3.2. PDV Setup

Two different PDV probes were used over the course of the experiments. The first was an off the shelf single point probe, while the second was a custom made multi point array. The single point probes had a key advantage of being much quicker and cheaper to obtain than the multi-point probes. This enabled initial testing and confirmation that the diagnostic worked while improvements were being made to the multi-point probes. The single point probes were CFS@-1550-APC from Thorlabs. This single point had a waist diameter of 0.39 μm and had a return loss of 55 dB. This high return loss is very useful as it creates very little to no reflected light from the probe itself which would result in an extended baseline, complicating the analysis. The large beam diameter is also advantages as it can keep a similar beam diameter over a long range as the divergence is relatively small, only 5.09 mrad. This means if the probe was 10 cm away from the load the beam diameter would be 640 μm, which is still within a 1 mm gap.

The multipoint probes were a fiber optic collimator array from OZ Optics. These arrays had 4 probes in a linear array with a center to center spacing of 250 μm and were collimated into a beam diameter of 120 μm. This arrangement therefor reaches the goal of having 4 points within 1 mm, as the end-to-end separation of the collection volume at the end of the probe is, 870 μm. In addition, these probes only had a return loss of 30 dB, creating a stronger extended baseline then the single point probes, which needed to be addressed during analysis.

A challenge however of using a small beam diameter for collimation means that the length that the spot could stay collimated for was relatively small. Looking to the Ryleigh length for the diffraction limit on the collimation gives a length of 7.3 mm. This means if we want to be able to keep resolution of the 4 fibers within the AK gap we would need to be close to within that range. To try to increase the longevity of a probe to be longer than a single shot significant protection of the probe was attempted.

The mount designed to hold the multi-point probe and increase the longevity is shown in Fig. 3-3. In addition, we added another 0.5" 1550 nm coated glass window, by screwing it to the front of the Thorlabs tube. To protect the fibers from debris we used metal braiding. And the vacuum fiber feed through was done with a KF50 vacuum hardware, sealed with Torr Seal epoxy resin.

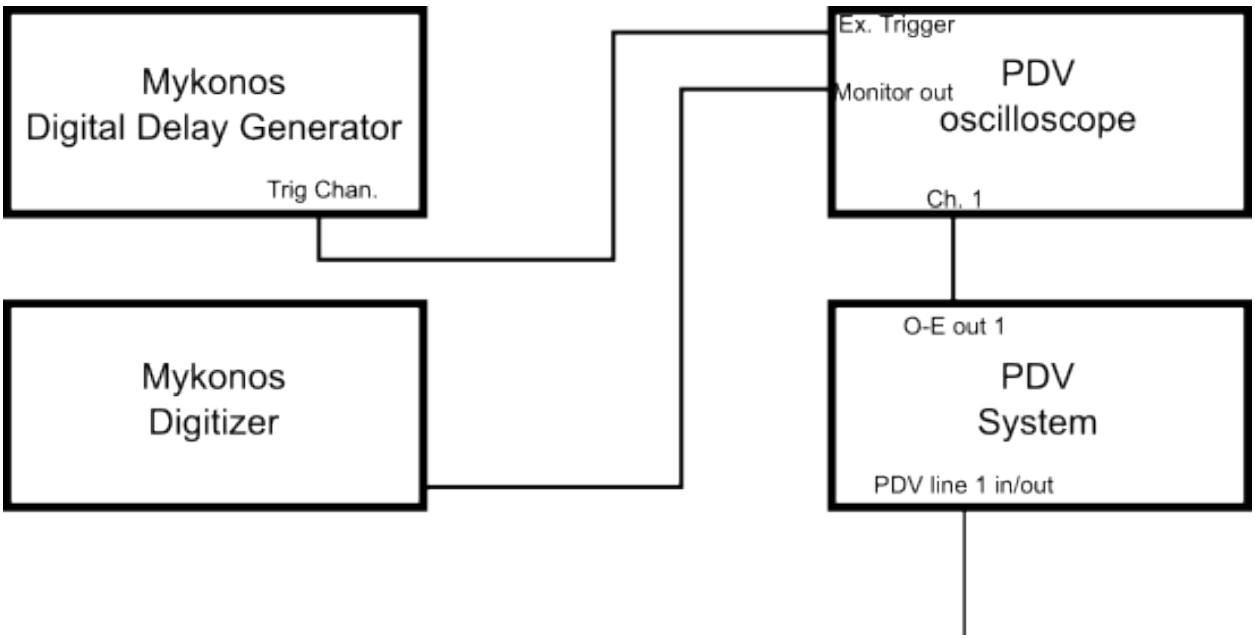

Figure 3-4 Diagram of the electrical and optical setup of the PDV system for a single channel.

In retrospective the effort to protect the fiber array was not useful, as the first array still had internal damage after the first shot. This damage was the lens array being separated from the fibers, and likely a result of a shock. In addition, the 1" tube hardware plus the glass windows played against the Ryleigh length and the optimal resolution for the array. With that in mind, for the second and third array shot we decided to use the fiber array with no protection whatsoever, which allowed the fibers to be placed much closer to the hardware.

The oscilloscope used for these experiments was DSOS804A from Keysight. This scope has 4 different channels and is capable of operating at 8 Ghz with 20 GS/s, however when more than 2 channels are used the frequency is reduced to 4 GhZ and only get 10 GS/s. These reduced specs were what we used when discussing the errors of this system.

The laser and the processing for the 4 PDV channels was able to be contained in a single NI PXIE-1084 box. Three different modules from QuanTiFi were used within this box for the PDV system. This included two laser modules, which each had 4 tunable lasers, 4 Dopplar modules which were used to combine the reference and signal lines together and effectively do the PDV, and 2 optical to electrical converters which converted the result to a signal that could be processed by the oscilloscope. These could all be driven by a SMASH program on a NI PXIe-8821 computer that was installed on the box. This enabled the PDV system to be completely controlled by a single box and oscilloscope system. A schematic of the PDV system connected to the Mykonos control and digitizer system is shown in Fig. 3-4

For both platforms the fiber was placed on one side of the experimental hardware and looked across the AK gap. Retroreflective tape was placed on the other side of the gap. This tape would reflect the light back along the same path and into the fiber that sent the signal. For the multi-point measurement, the laser wavelength of each channel was separated by 1 nm which prevented cross

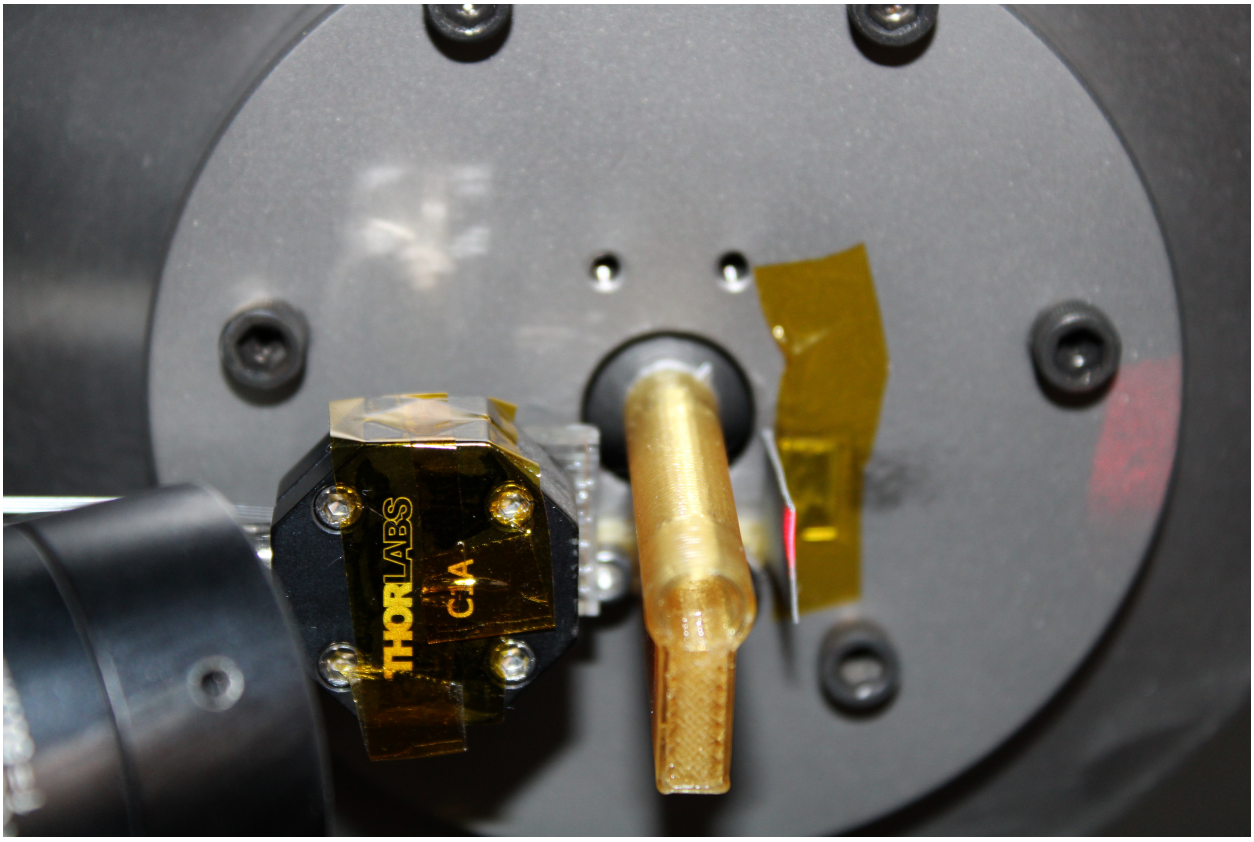

Figure 3-5 Shows the multi-point PDV probe setup on thin foil experiments. Left is the PDV probe, middle is the thin foil holder, and right is the retroreflective tape.

talk between the 4 different channels. A sample of this setup with the multi-point probe on the thin foil experiments is shown in Fig. 3-5.

This page left blank

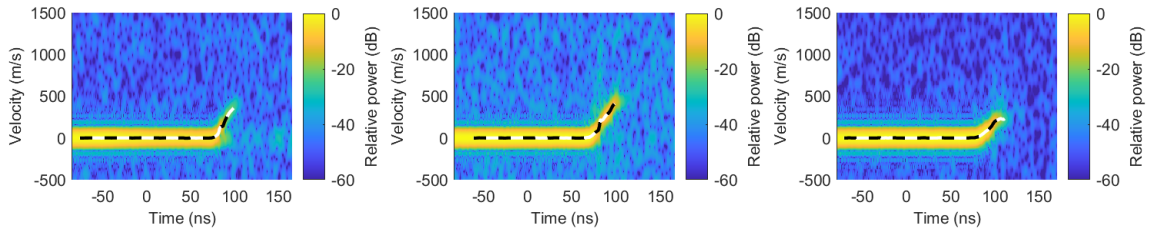

Figure 4-1 The spectrographs from the three thin foil experiments with the baseline removed. left) 100 μm stainless steel. middle) 200 μm stainless steel. right) 300 μm aluminum. The dashed line shows the measured apparent velocity from the PDV signal.

4. RESULTS

As discussed in the previous section, data was collected on two different experimental platforms during this LDRD that are relevant to power flow plasmas. The first platform was a thin foil experiment that was developed to help study power flow relevant physics on smaller scale machines. This platform was first used on the MAIZE facility and has recently been used on the Mykonos machine [8]. In addition, the Mykonos parallel plate platform (MP3) was also used [6]. This platform enables the current density to reach levels comparable to the inner MITL on Z which makes it a good platform for studying power flow physics. Both platforms have a clear line of sight into the power flow region, which make them great options for developing new diagnostics.

4.1. Thin Foil Experiments

The first set of experiments was on the thin foil platform. On the first set of these experiments single point measurements were gathered on three different current pulses around the center of the AK gap. These were all single point measurements to perform initial testing of the system. One of these measurements was done with the multi-point probe, however only one channel was saved, so even that was a single point measurement. Even though the goal of this project is for multi-point measurements, using single point measurements enabled checking that this diagnostic technique worked on Mykonos.

The three shots for the single point measurements were using 100 μm stainless steel, 200 μm stainless steel, and 300 μm aluminum foil. The spectrographs for these three shots, using a 10 ns STFT, are shown in Fig. 4-1. We will note that the 100 μm stainless steel shot used the multi-point probes that were discussed, while the other two shots used single point probes. The multi-point probe causes a strong baseline after the main experiment due to having a high back reflection in the probe, 30 dB, and the fact that multiple windows were placed in front of the probe, all increasing the amount of back reflection in the probe. Even with this strong baseline the primary signal was still apparent. While the baseline was removed for this figure and analysis the effects of removing the baseline on the results will be discussed later, but this can be performed in SMASH. All three experiments show a clear increase in the velocity between 70 and 100 ns into the current rise before the shifted signal dies away.

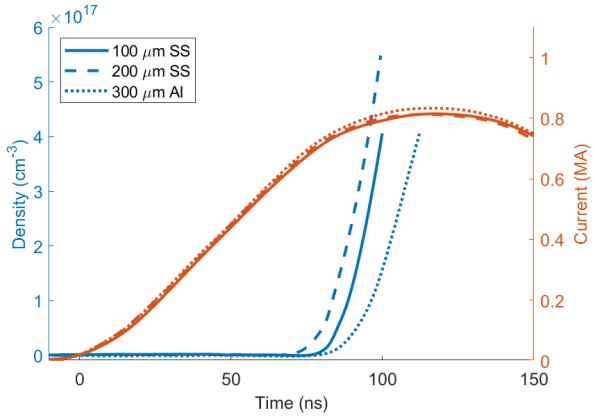

Figure 4-2 Results for the density as measured by PDV on the 3 single point thin foil experiments. The measured density is shown in blue and the measured current in orange. Time is adjusted so that time=0 occurs when the current reaches 20 kA. We see differences in the measured density between the three different loads

The apparent velocities from these spectrographs can then be integrated to find the density, and the results are shown in Fig. 4-2. We see that the measured density starts to pick up around 70-80 ns into the current rise. The measurement then stops around 100 to 110 ns into the current pulse, which is around peak current. This stopping point seems to occur when the density is in the mid to upper 10^{17} cm^{-3}. The fact that the probes seem to fail as a detector at this point is interesting, as this is well below the critical density of 4.6×10^{20} cm^{-3}. Even though this is well below the critical density, it does appear to give a strong indication of density in the AK gap for these foil liners.

There are several possible explanations for the failure of the diagnostic significantly before the critical density is reached [3]. One explanation is that most of the 1 cm plasma path is actually lower density plasma and there are smaller high-density regions. These high-density regions would block the laser, but the average density would still be significantly below the cutoff frequency. Another effect could be local density gradients deflecting the collimated laser beam, causing it not to go back into the fiber. The hope however is that by using retroreflective tape the effects of beam steering should be minimized. Another concern is that ions and neutrals can increase the refractive index [4, 7]. This can go so far to cause an index of refraction greater than one. We note that at no time in these three experiments did we see an index of refraction greater than one, but these effects could still be reducing the inferred electron density. A way to remove this source of error would be to expand to a two-color system, enabling a comparison of two different calculations of the index of refraction. A fourth source of error could be some error in the optics path itself. This could be due to the optic in front of the fiber getting either so coated or blanking to no longer transmit light. In addition, the retroreflective tape was just taped to the hardware, and if the forces were strong enough to blow it out of the optics path, we would no longer receive signal. More exploration will be needed to fully understand what is causing this relatively early failure of the diagnostic, and if it has any impact on the interpretation of the data. However, the data still provides good hope for this diagnostic.

One thing that can be done in the processing of the signals is removing the extended baseline.

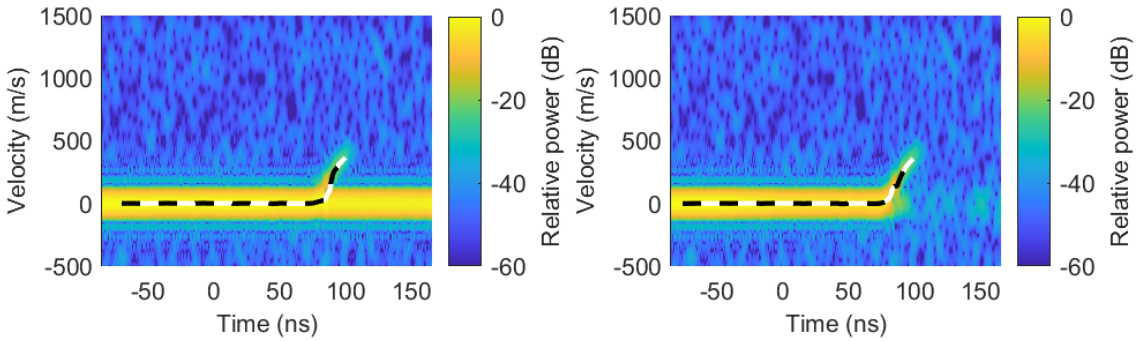

Figure 4-3 Comparison of the spectrographs with the baseline removed for the strong baseline shot. left) shows the spectra with the baseline and right) shows the same spectra with the baseline removed.

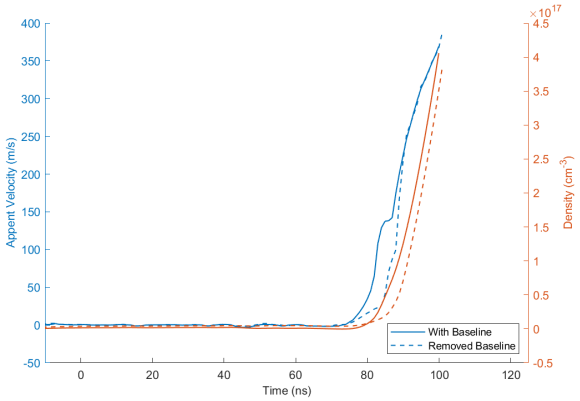

Figure 4-4 Comparison of the density with removing the baseline, we see a slight change at the start of the density rise, which makes sense as that is likely where the baseline interferes the most.

This is extremely important in shots with strong baseline such as the 100 μm stainless steel shot. We can see a comparison of the two spectrograms in Fig 4-3 and the measured velocities and the calculated densities in Fig 4-4. We see that in the results the major region for disagreement is right when velocity begins to come above 0. This error in the non-baseline removed case is because the trace is fitting to the baseline instead of the actual signal. By removing the baseline, we are better able to measure the actual signal. We can see in this case the error caused by not removing the base line caused the density to be underestimated by 3×10^{16} cm^{-3}.

On a later campaign a single shot was performed using a multi-point probe on these thin foil experiments. The load for this experiment was 200 μm thick Aluminum foil. The probe was placed so that the lowest fiber was just off of the anode, and then the other probes were aligned just above that to see about a mm above the anode, with the alignment of this probe being shown in Fig 4-5. We can see the spectrograph results from this shot in Fig. 4-6. As this is the multi-point probe, we do see a significant amount of an extended baseline. There is an additional challenge with this baseline as it is not at all flat or even, making it basically impossible to remove. Therefore, it makes it challenging to distinguish the measured signal from the baseline, especially at small velocities, increasing the error in the inferred electron density. In addition the seems to be several artifacts in the data, making deciphering the true signal challenging. The density results for the best attempt at measuring these apparent velocity's are shown in Fig. 4-7. Sadly, the

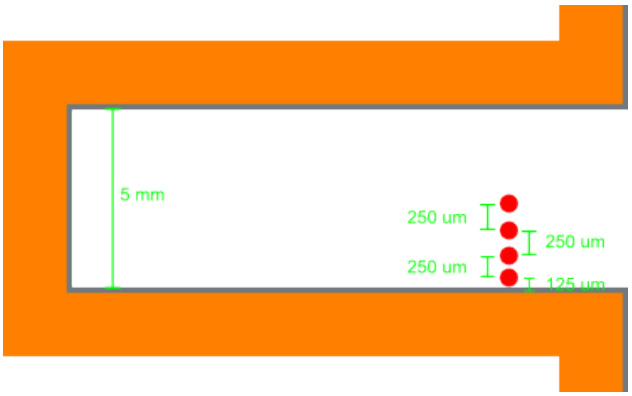

Figure 4-5 Diagram of the alignment of the PDV probe for the thin foil experiments. Note the lowest probe was adjusted so it was just clearing the surface. The diameter of each PDV measurement was about 120 μm. (figure not to scale.)

interpretation of this data is relatively confusing as there is no obvious time correlation in the different measurements. We expect to see plasma expanding from either the cathode or the anode, meaning that the density should be increasing across the probes in one direction. Instead, we see one of the middle fibers reaching high density first, and the other middle fiber reaching high density last, with a time separation on the order of 10 ns. If we look at the plot of the velocity and density, we see this time shift throughout the velocity measurements, and not just at early times when we are close to the base line, suggesting this might not be just an error in tracing the velocity due to the strong background. The fiber lengths were well characterized as well as timing delays of the PDV system, so we do not expect this timing difference to be due to systematic errors in the timing. This is interesting as we don't seem to have a clear direction of plasma expansion into the gap region, from either the anode or the cathode.

4.2. MP3 hardware

We also fielded the multi-point diagnostic on a single shot with the MP3 hardware. The cathode size was 1.5 mm x 1.0 mm, with an AK gap spacing of 1 mm. The probe was set up to look across the AK gap just off of the knee of the anode. The alignment was done following the same method as for the thin foil experiments and shown in Fig. 4-5, but now with only a 1 mm gap. The alignment of the probe along the AK gap was found by seeing where the red alignment laser would hit the anode, and for this shot is shown in Fig. 4-8. We did verify that light was going through the gap for all 4 fibers.

The spectrographs for this shot are shown in Fig. 4-9. We will note that as these were the multi-point probes they had a strong baseline, however this time it was even enough that it could be removed, which was what was down for the two probes close to the anode. There are clear measurements of an apparent velocity on both probes 3 and 4, which were the closest two to the anode. The measured densities from this experiment are shown in Fig 4-10. Comparing these 4 measurements shows several interesting features. First, fibers 3 and 4 agree in the measured density for most of the density rise, except for right at the end of the probing window. This strong agreement between these two probes could suggest that the density being measured is primarily

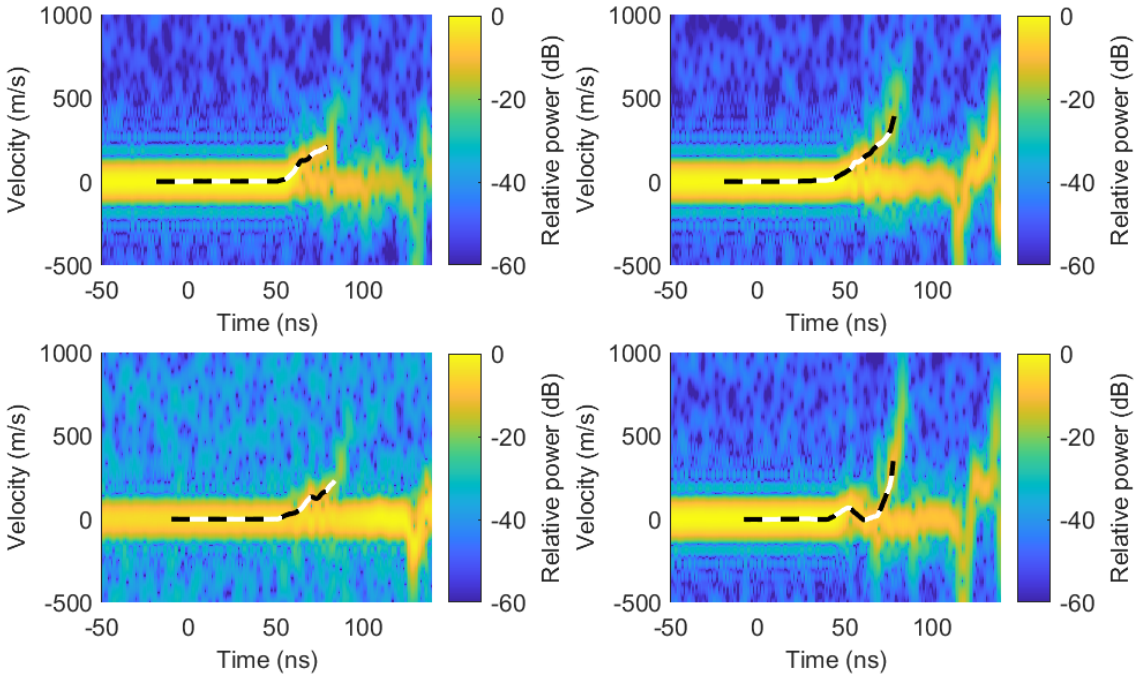

Figure 4-6 The spectrographs from the multi-point measurements on the thin foil platform. a) fiber 750 μm from anode b) fiber 500 μm from anode c) fiber 250 μm from anode d) fiber aligned to the edge of anode. The dashed line shows the measured apparent velocity from the PDV signal.

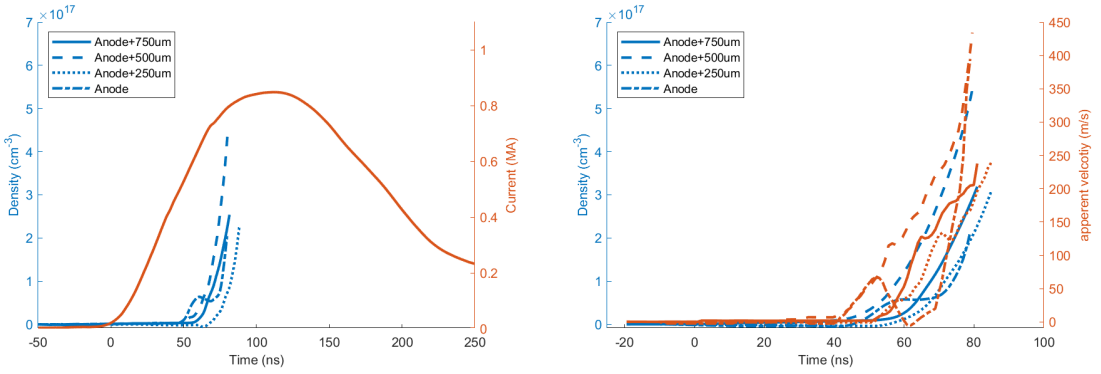

Figure 4-7 left) Measurements of the density from the multi-point measurements for a 200 μ thin foil experiment. All 4 fibers appear to have a different start time for the rise in density, which does not seem to follow a location trend. right) Comparison of the density and the velocity measurement of the 4 probes.

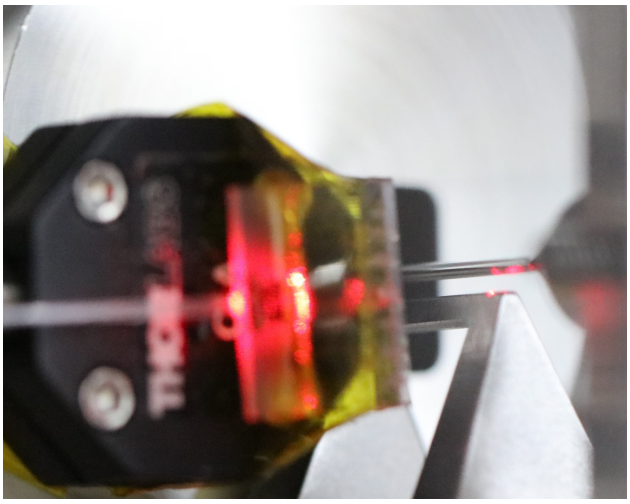

Figure 4-8 Alignment of the PDV hardware for the shot on the MP3 hardware. We see the laser hitting just inside the knee on the anode surface.

being swept along in the experiment and gathering here at the anode knee, rather than expanding from the anode at this location. We also note that there is very little analyzable signal in channel 2 and none in channel 1. This would seem to suggest then that most of our plasma is closer to the anode, which seems to agree with shadowgraph and self-emission of similar types of loads, which shows very large amount of plasma right on the knee [6].

Another interesting thing to note is that, while we still are well below the cutoff frequency, we get to a much higher density then what was seen in the thin foil experiments. We note that the path length for the PDV measurement on the MP3 platform is only 2 mm compared to the 10 mm length of the thin foil platform. This means that a comparable velocity shift will result in a higher density. Even with that in mind we are still reaching higher areal densities then seen in the thin foil experiments, at least on the probes closest to the anode. Also, the time until probe failure is significantly longer than in the thin foil experiments, being over 100 ns in this case compared to about 30 ns in the case of the thin foil experiments. While more exploration is still needed here, these differences in when the probes fail could help to provide insights into how we can get this measurement closer to the critical density, or at least understand why we are not reaching it.

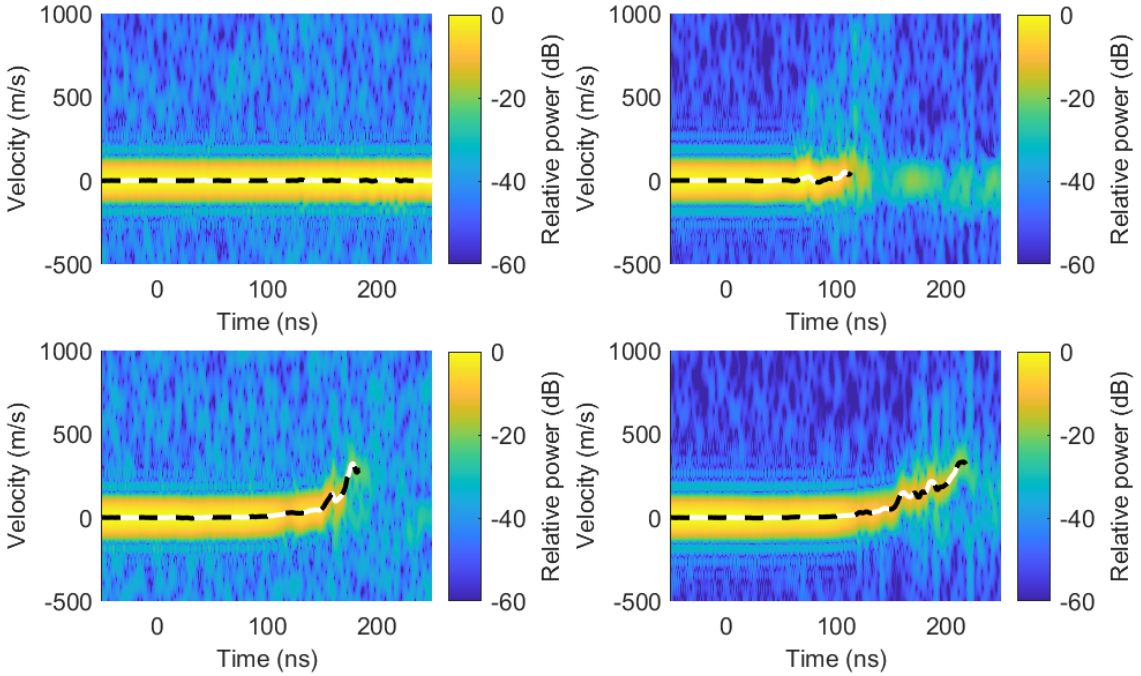

Figure 4-9 The spectrographs from the multi-point measurements on the MP3 platform. a) fiber 750 μm from anode and close to the cathode b) fiber 500 μm from anode c) fiber 250 μm from anode d) fiber aligned to the edge of the anode. The dashed line shows the measured apparent velocity from the PDV signal. We see more apparent velocity close to the anode.

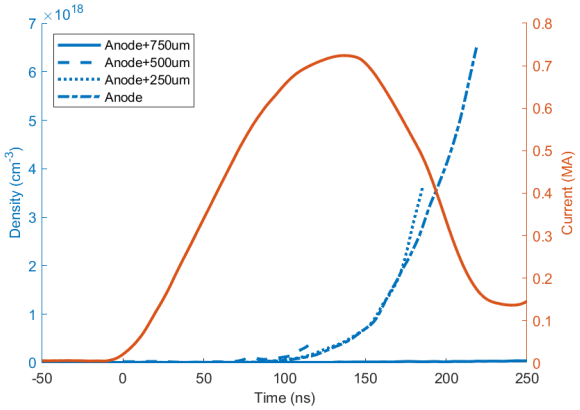

Figure 4-10 Measurements of the density from the multi-point PDV diagnostic for the MP3 hardware. We see significant density measurements on the 2 fibers closest to the anode, which seem to be in good agreement.

This page left blank

5. CONCLUSION

A PDV diagnostic was developed to measure the electron density with both temporal and spatial resolution for power flow plasmas. This was a combination of single point measurements to test the system and then several multi-point measurements, and measurements were performed on both the thin foil and MP3 platform. The single point measurements were very successful, showing clear increase in density just before peak current. The multi-point measurements however were less clear, likely due to strong baseline effects. They did seem to show at least some density. In addition, one of the early measurements was performed with the same type of probe as the multi-point measurement, suggesting with improvements to the final experiments this diagnostic would be in a good place for power flow plasmas.

5.1. Next steps

One of the big challenges of these experiments was finding a good arrangement for the multi-point probe. And while we did see some promising initial results from the probes used in these experiments, there was challenges with the probes both in analyzing the data and fielding them that could be improved on future iterations of the project. One of the challenges with these multi-point probes was the fact that the return loss of the probe was 30 dB, creating a strong baseline signal. The single point probes were much better than this at 50 dB and much easier to analyze. Therefore, in the future, it would be desirable to have a multi-point measurement with a larger return loss value. In addition, to keep the desired spatial resolution these probes were needed to be relatively close to the target. This caused the probe to be damaged and needed to be replaced every shot, which considering the cost of these probes is likely not sustainable for a long-term diagnostic. One possible future improvement would be to use MTP/MPO connectors as the array of fibers and then use a lens to focus them at the load. This would enable significantly more standoff which would better protect the probe as well as reduce the risk of the probe interfering with the experiment. This set up would likely use a large diameter lens to focus the fibers into the center of the AK gap. This would need to be performed at a magnification of 1 in order to keep the 4 fibers within the 1 mm gap but would also allow for flexibility in the design if a different gap size was being measured. We will note that the 1 magnification would lead to a relatively tight focus in the gap and therefore will not stay small for long. This may cause a problem for wider platforms such as the thin foil experiments, but they likely would desire a larger field of view then 1 mm, which would help on this problem.

Another thing to note is that the later experiment, with the multi-point probes, had complication with background signal that were not present in the earlier shots, even when a strong background was present. One possible cause for this was a change in how the fiber was set up as shown in Fig. 5-1. We are now concerned that the second setup using the long thin rod could have led to more vibrations of the probe. This vibration of the probe could be a cause of the complex baseline after the shot. Therefore, future designs would need to keep this in mind and avoid large lever arms that might lead to large vibrations.

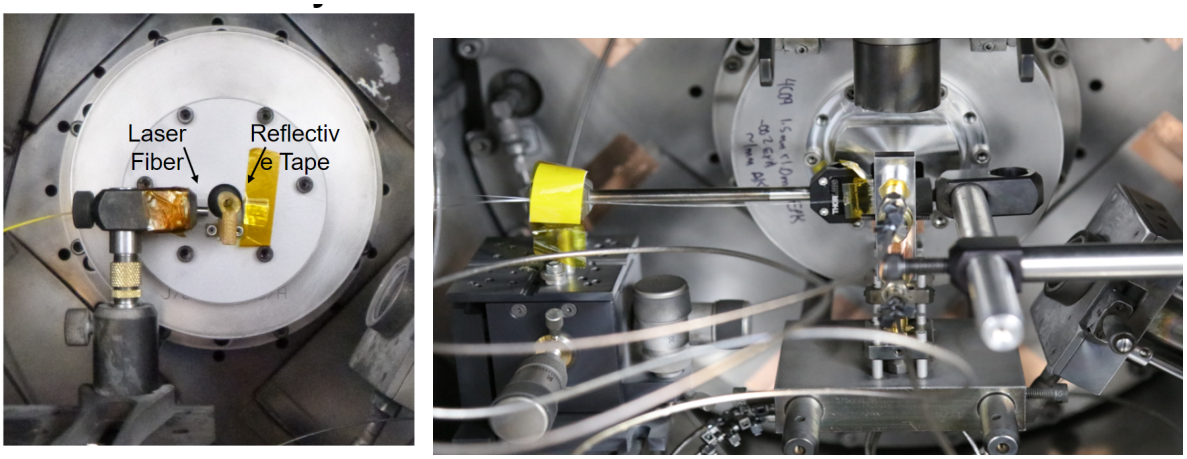

Figure 5-1 left) setup for original single point measurements. right) setup for the later multi-point probe measurements. We see that the later probe has a long arm that could be acting as a lever arm, creating vibrations.

Finally, if this is going to become a future routine diagnostic on Mykonos design improvements will likely be needed to improve the speed of install and alignment, so it could be routinely fielded with less of an impact to each shot. Currently installing and aligning the fiber takes around 2 hours per shot. Ways that this could be improved in the future would be to use better protected fibers such as through jacketing, which would make loading into the chamber easier. In addition, getting a common vacuum connection port would enable easier changing of fibers after each shot.

Another possible future improvement would be to expand this system to a two-color PDV system. This was discussed earlier, but it could remove some of the challenges of processing and interpreting the interferometer signal as there would be two different dispersion relations. This would help enable distinguishing from a possible positive shift in the index of refraction caused by the ions and neutrals in the plasma. While 1550 nm is very convenient for PDV systems, due to is large use in the telecom industry, other wavelengths can be considered, such as 1310, 1064, 755, or 532 nm, but each would present their own set of challenges[2].

REFERENCES

[1] D. H. Dolan. Accuracy and precision in photonic doppler velocimetry. *Rev Sci Instrum*, 81(5):053905, 2010.

[2] D. H. Dolan. Extreme measurements with photonic doppler velocimetry (pdv). *Rev Sci Instrum*, 91(5):051501, 2020.

[3] D. H. Dolan, K. Bell, B. Fox, S. C. Jones, P. Knapp, M. R. Gomez, M. Martin, A. Porwitzky, and G. Laity. Plasma and radiation detection via fiber interferometry. *Journal of Applied Physics*, 123(3), 2018.

[4] J. Filevich, J. J. Rocca, M. C. Marconi, S. J. Moon, J. Nilsen, J. H. Scofield, J. Dunn, R. F. Smith, R. Keenan, J. R. Hunter, and V. N. Shlyaptsev. Observation of a multiply ionized plasma with index of refraction greater than one. *Phys Rev Lett*, 94(3):035005, 2005.

[5] N. R. Hines, Sonal Patel, Daniel Scoglietti, Mark Gilmore, S. L. Billingsley, R. H. Dwyer, Thomas Awe, Darrell Armstrong, David Bliss, George Laity, and Michael Cuneo. A fiber-coupled dispersion interferometer for density measurements of pulsed power transmission line electron sheaths on sandia's z machine. *Review of Scientific Instruments*, 93(11), 2022.

[6] D. C. Lamppa, S. C. Simpson, B. T. Hutsel, G. Laity, M. E. Cuneo, and D. V. Rose. Assessment of electrode contamination mitigation at 0.5 ma scale. 2021.

[7] Joseph; Nilsen and Walter R. ; Johnson. Plasma interferometry and how the bound-electron contribution can bend fringes in unexpected ways. *APPLIED OPTICS*, 44(34):7295, 2005.

[8] T. J. Smith, P. C. Campbell, G. V. Dowhan, N. M. Jordan, M. D. Johnston, M. E. Cuneo, G. R. Laity, and R. D. McBride. Additively manufactured electrodes for plasma and power-flow studies in high-power transmission lines on the 1-ma maize facility. *Rev Sci Instrum*, 92(5):053550, 2021.

[9] O. T. Strand, D. R. Goosman, C. Martinez, T. L. Whitworth, and W. W. Kuhlow. Compact system for high-speed velocimetry using heterodyne techniques. *Review of Scientific Instruments*, 77(8), 2006.

[10] K. J. Swanson, G. S. Jaar, D. C. Mayes, R. C. Mancini, V. V. Ivanov, A. L. Astanovitskiy, O. Dmitriev, A. W. Klemmer, C. De La Cruz, D. Dolan, A. Porwitzky, G. P. Loisel, and J. E. Bailey. Development and integration of photonic doppler velocimetry as a diagnostic for radiation driven experiments on the z-machine. *Rev Sci Instrum*, 93(4):043502, 2022.

This page left blank

DISTRIBUTION

Email—Internal

Name	Org.	Sandia Email Address
Jacob Banasek	1659	jtbanas@sandia.gov
Pablo Reyes	1659	pareyes@sandia.gov
Dan Dolan	1646	dhdolan@sandia.gov
Jens Schwarz	1659	jschwar@sandia.gov
Mike Cuneo	1650	mecuneo@sandia.gov
Keith Matzen	1000	mkmatze@sandia.gov
Greg Frye-Mason	1370	gcfrye@sandia.gov
Technical Library	1911	sanddocs@sandia.gov

Hardcopy—Internal

Number of Copies	Name	Org.	Mailstop
1	L. Martin, LDRD Office	1910	0359

This page left blank

Sandia National Laboratories is a multimission laboratory managed and operated by National Technology & Engineering Solutions of Sandia LLC, a wholly owned subsidiary of Honeywell International Inc., for the U.S. Department of Energy's National Nuclear Security Administration under contract DE-NA0003525.